Matrix Infrared Study of O-Initiated Atomic Oxidation of CH_3Cl: Identification of the Triplet $CH_3Cl\cdots O$ Complex

L. Schriver-Mazzuoli* and A. Schriver

Laboratoire de Physique Moléculaire et Applications,† Laboratoire propre du CNRS, UPR 136, Université Pierre et Marie Curie, Tour 13, case 76, 4 place Jussieu, 75252 Paris Cedex 05, France

Y. Hannachi

Laboratoire de Physicochime Moléculaire (CNRS UMR 3805), Université de Bordeaux I, 351 Cours de la Libération, 33405 Talence Cedex, France

Received: July 2, 1998; In Final Form: October 7, 1998

Infrared spectroscopic studies have been conducted on the products of the reaction between atomic oxygen in its ground and excited states with normal and isotopically substituted methyl chloride in argon matrixes at 11 K. With the $O(^1D)$ atom, the major product is the hydrogen-bonded complex between formaldehyde and hydrogen chloride. Abstraction of a hydrogen atom from CH_3Cl by $O(^1D)$ appears as a minor channel. Small amounts of HClCO were also found. Formation of CO−HCl as a secondary and primary product was observed. Reaction of CH_3Cl with the $O(^3P)$ atom was evidenced. Spectra suggest the formation of a collision complex $CH_3Cl\cdots O$ formed by addition of an oxygen atom to CH_3Cl. Ab initio calculations about the structure and vibrational spectrum of the CH_3ClO singlet and $CH_3Cl\cdots O$ triplet are reported.

1. Introduction

The flux of halogen-containing species into the lower stratosphere depends on the tropospheric oxidation of halogenated compounds. Recently, numerous studies supported by AFEAS (Alternative Fluorocarbons Environmental Acceptability Study) and the European Community have been devoted to the atmospheric degradation mechanisms for various halogenated compounds in order to determine the effect of releases of future man-made compounds into the stratospheric ozone layer and to provide a significant input into legislative controls on the use of these compounds. In particular, attention was turned on halocarbons containing hydrogen atoms, which may be degraded in the troposphere by reaction with hydroxyl radicals.[1−3] Investigations of the reactions of produced haloalkyl, haloalkoxy, and haloalkylperoxy radicals with NO_2, NO_3, and O_3 were performed.[4−8] With less importance, oxidation of halogenated organic compounds in the troposphere can occur from their reaction with atomic oxygen in ground and excited states, although the concentration of $O(^1D)$, which is a key compound in the lower stratosphere and the troposphere, depends critically on the absorption by ozone of radiations with wavelength around 310 nm. There is little available data in the literature on the oxidation of halogenated methane compounds by atomic oxygen. Recent study on the photooxidation mechanisms of CH_3Cl, CH_3Br, $CHBr_3$, and CF_3Br in dry air between 180 and 400 nm mentioned the formation of CH_2Cl and CH_2Br radicals by abstraction of a hydrogen atom by an oxygen atom.[9] To obtain some information about the photooxidation mechanism of chloromethanes by atomic oxygen, we have undertaken for 5 years in this laboratory a systematic study of the photoreaction of ozone with various chloromethane species using the matrix isolation technique in conjunction with FTIR spectroscopy.[10−14]

Although the matrix technique, which involves condensing the species to be studied with an excess of inert gas at low temperature, requires experimental conditions very different of those of atmosphere, it can readily be well adapted in some aspects of atmospheric chemistry research such as, for example, elucidating the structures of transient species and reactions intermediates, preventing the occurrence of any process with an activation energy of more than a few kilojoules per mole, and studying the structure and photochemistry behavior of specific molecular complexes. Furthermore, photolysis under matrix condition is likely to provide a better model than the gas phase of the effects of photolysis on species in polar stratospheric clouds or aerosols. Studies of the reation between oxygen atoms generated by ozone photolysis and $CHCl_3$,[10] $CBrCl_3$,[11] $CFCl_3$,[12] CH_2Cl_2,[13] CCl_4, CH_3CCl_3,[14] and CBr_3F[15] in an argon matrix showed mainly the formation of carbonyl compounds with concomitant abstraction of HCl, BrCl, Cl_2, or Br_2 for hydrogen-containing species. However, no intermediate was evidenced. To rationalize our previous observations and to determine possible reaction intermediates, the present work concerns the investigation of oxygen-initiated photooxidation of methyl chloride in argon.

Methyl chloride is the most nonindustrial chlorocarbon species in the atmosphere, although a significant urban source of CH_3Cl exists probably due to automobile exhaust. It is mainly formed in seawater by chloration of CH_3I, which is produced by marine algae and by smouldering burning of vegetation. Its mixing ratio in the atmosphere is 0.5/1 ppb, and its lifetime is 2−3 years.

2. Experimental Section

All the experiments conducted in the present study were carried out on a matrix isolation apparatus that has been described previously.[10] Normal methyl chloride (Matheson) and

* To whom correspondence should be addressed.
† Laboratoire Associé aux Universités P. et M. Curie et Paris-Sud.

10.1021/jp9828538 CCC: $15.00
Published on Web 11/21/1998

deuterated methyl chloride (Eurisotop-CEA) were degassed to −196 °C on a vacuum line before use, then distilled from −20 °C for preparing the matrix mixture. Oxygen atoms (^{16}O and ^{18}O) were produced in situ from the photolytic decomposition of ozone trapped in the matrix. Consequently, ozone was prepared from natural oxygen (Air Liquide N50) and $^{18}O_2$ mixtures (Eurisotop CEA) contained in a glass vacuum finger excited by a Tesla coil discharge and trapping at liquid nitrogen temperature. Residual oxygen was removed by freeze−pump−thaw cycles with liquid nitrogen.

Samples (CH_3Cl/Ar and O_3/Ar) were deposited from two separate inlets onto a gold plated mirror at a rate of 10^{-2} mol/h. A temperature controller (Silicon diode 9600-1) was used to maintain the chosen temperature to within ±0.1 K. The deposition temperature was 20 K, and the recording temperature was 11 K. Argon (Air Liquide N 56) was used without further purification. Infrared spectra were recorded over the 4000−400 cm^{-1} range in a reflection mode using a fourier transform infrared spectrometer (Bruker IFS 113 v) with a resolution of 0.5 cm^{-1}. The optical path between the beam extraction and the cryostat was nitrogen purged to avoid atmospheric absorption by CO_2 and H_2O. The photolysis of ozone was carried out by irradiating the samples with the 532 nm second harmonic and the 266 nm fourth harmonic of a Nd:YAG laser (Quantel YG 781 20 C). The initial laser power was 10 or 20 mJ in each case. To obtain an unfocused beam, the light intensity was spatially homogenized with a fluorine lens.

3. Vibrational Spectra of Parent Molecules

Infrared spectra of isotopic and natural ozone species have been widely studied in the gas phase and in various matrixes (ref 16 and references therein). In solid argon, natural ozone (666) is characterized by doublets in each fundamental region. The most intense components of each doublet are measured at 1104 (ν_1), 700 (ν_2), and 1039 cm^{-1} (ν_3) and show an intensity ratio of $\nu_1/\nu_2/\nu_3 = 0.07/1/13$.

The C_{3v} methyl chloride molecule has nine normal modes of vibration, three modes of A_1 symmetry, and three E degenerated modes. The infrared spectra of hydrogenated and totally deuterated methyl chloride in the gas phase were described 25 years ago by Tanabe et al.[17] More recently, as a result of the importance of CH_3Cl in the atmosphere, many infrared investigations at high resolution including measurements of band strengths and the far-infrared region have been reported.[18−21] In matrixes, relatively little is known about the spectrum of CH_3Cl. Only an analysis of the $^{35}Cl-C$ and $^{37}Cl-C$ stretching modes in the argon matrix was reported by King.[22] Consequently, we have recorded spectra of hydrogenated and deuterated methyl chloride diluted in argon ($M/A = 1/1000$). The positions and approximate relative intensities of absorptions characterizing the fundamental modes are summarized in Table 1 and compared with gas-phase data. Figure 1 illustrates the chlorine isotopic dependence of ν_{CCl} infrared absorption for both CH_3Cl and CD_3Cl. Measured positions of the doublet components (722.4−716.7 and 692.5−686.1 cm^{-1}) indicate a 5.7 and 6.4 cm^{-1} separation of the pair of absorptions, respectively. The intensity ratio of the components (1/3) and the 6 cm^{-1} average value are in agreement for a CCl stretching mode of a species containing a single chlorine atom. This observed difference between the separation for CH_3Cl and CD_3Cl can be qualitatively understood by considering the heavier deuterium to damp the carbon motion and thus to increase the relative contribution of the chlorine mass to the reduced mass of the vibration, as previously observed for the CH_2Cl radical.[23] Other A_1 absorptions appeared, as expected, as single bands, but some E absorptions showed a doublet structure insensitive to temperature effects.

TABLE 1: Comparison of Fundamental Vibration Frequencies (in cm^{-1}) for Isotopic Methyl Chloride in Vapor Phase and Argon Matrix

	CH_3Cl			CD_3Cl	
modes	gas	Ar matrix		gas	Ar matrix
	a	*b*	this work	*a*	this work
A_1					
ν_1 ($\nu^s_{CH_3}$)	2976		2965.1	2155.0	2156.5
ν_2 ($\delta^s_{CH_3}$)	1355		1349.4	1028.0	1023.1
ν_3 (ν_{CCl})	728	722.5 (^{35}Cl)	722.4	683.0	692.5
		716.9 (^{37}Cl)	716.7		686.1
E					
ν_4 ($\nu^a_{CH_3}$)	3043		3040.8	2280.0	2280.9[c]
ν_5 ($\delta^d_{CH_3}$)	1453		1445.5[d] (sh)	1048.0	1054.8[e]
ν_6 (r_{CH_3})	1018		1015.0	760.0	765.3

[a] Reference 17. [b] Reference 22. [c] Shoulder to 2279.5 cm^{-1}. [d] Shoulder to 1448.0 and 1443.9 cm^{-1}. [e] Shoulder to 1055.5 cm^{-1}.

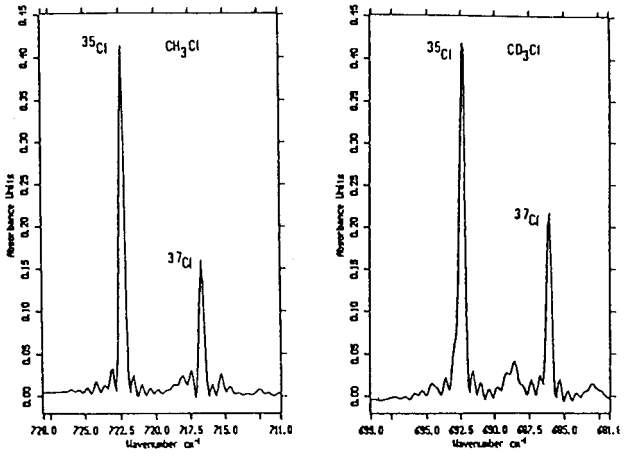

Figure 1. FTIR spectra of CH_3Cl and CD_3Cl in an argon matrix in the ν_{C-Cl} stretching region ($CH_3(D_3)Cl$/Ar1/1000).

Some harmonic and combination bands were also observed. Their positions are summarized in Table 2 as well as the anharmonicity coefficient values x_{ii} and x_{ij} calculated from the well-known equations

$$2x_{ii} = 2\nu_i - \nu_{2i}$$

$$x_{ij} = (\nu_i + \nu_j) - \nu_{i+j}$$

4. Photolysis of $CH_3(D_3)Cl/O_3$/Ar Mixtures

Two kinds of photolysis experiments were performed at 10 K. In the first set, irradiation was carried out with the 266 nm laser line. In the second set, irradiation was made with the 532 nm laser line. Under 266 nm irradiation, dissociation of ozone produces atomic oxygen in the $O(^1D)$ excited state and the $O(^3P)$ ground state, with a primary quantum yield of 0.83 and 0.17, respectively. In an argon matrix, recombination of $O + O_2$ occurs, but thanks to the cage exit of oxygen atoms, a decrease of ozone is observed.[24] Irradiation of ozone at the 532 nm laser line leads only to ground state atomic and molecular oxygen, but in matrix, the two photofragments recombine and only a very weak decrease of ozone is observed after a long irradiation time.[25] However, upon temperature increase, diffusion of $O(^3P)$ can be expected over a short range.[26] Consequently, experiments with the 532 nm laser line were performed to 25 K in order to allow a possible reaction between $O(^3P)$ and CH_3Cl in molecules that are nearest neighbors.

TABLE 2: Anharmonicity Coefficients of CH_3Cl and CD_3Cl in Argon Matrix Obtained from Observed and Calculated Frequencies of Some Harmonic and Combination Bands

	calculated	observed	x_{ii}	calculated	observed	x_{ij}
			CH_3Cl			
$2\nu_3$	1444.8, 1433.3	1435.7, 1424.5	4.5, 4.4			
$\nu_2+\nu_3$				2071.9, 2066.1	2064.5, 2058.5	7.5, 7.2
$\nu_2+\nu_6$				2364.4	2359.2	5.2
$\nu_5+\nu_6$				2460.5	2454.1	6.5_5
			CD_3Cl			
$2\nu_3$	1385.0, 1372.2	1377.3	3.8_5			
$2\nu_5$	2109.4	2105.9	1.8			
$\nu_2+\nu_3$				1715.6, 1709.2	1710.5, 1704.3	5.0_5, 4.8_5
$\nu_2+\nu_6$				1788.4	1783.4	4.9_5
$\nu_5+\nu_6$				1820.1	1817.8	2.2_5

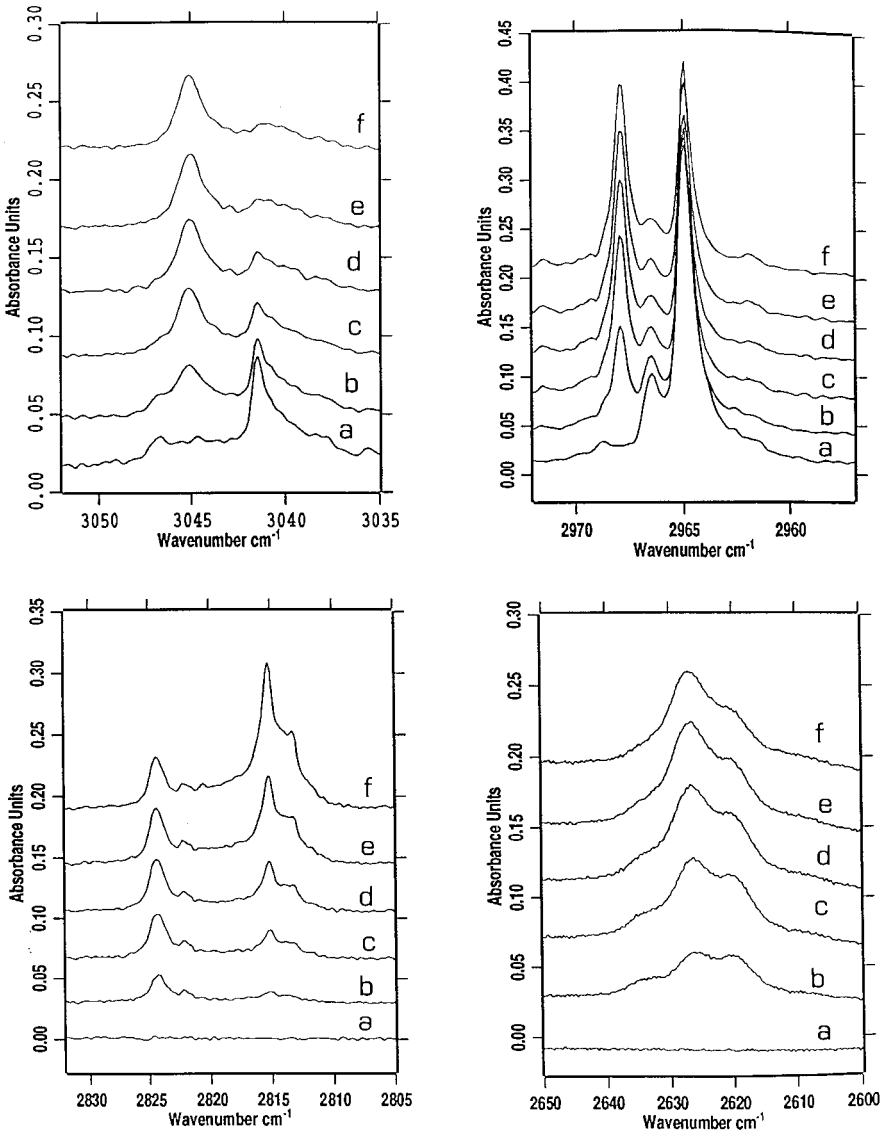

Figure 2. Product band growth during laser photolysis of a $CH_3Cl/O_3/Ar1/2/1000$ mixture in typical spectral regions above 2000 cm^{-1} with photolysis times of (a) 0, (b) 10, (c) 30, (d) 60, (e) 120, (f) 240 min.

The matrix ratios for ozone and methyl chloride in argon were typically 1/500 and 1/500. To help with the assignment of product reaction bands, CD_3Cl and isotopic 18 ozone were also used.

4.1. Irradiation with the 266 nm Laser Line. Irradiation of the matrix for a total of 120 min ($F = 1.3\ 10^{17}$ photons cm^{-2} s^{-1}) totally destroyed the ozone and about 40% of methyl chloride. The photolysis of the two parent molecules was accompanied by the appearance of numerous bands throughout the 3000−700 cm^{-1} spectral range. Figures 2 and 3 show some key spectral regions after different irradiation times. The absorption frequencies and approximate intensities of all the features produced during photolysis are summarized in Table 3 with the lines observed in $CDCl_3$ and $^{18}O_3$ experiments.

4000−3000 cm^{-1} Region. A weak new band, which did not seem to belong to water traces, appeared at 3352.5 cm^{-1} in the ν_{OH} region and shifted to 3341.0 cm^{-1} in $^{18}O_3$ experiments.

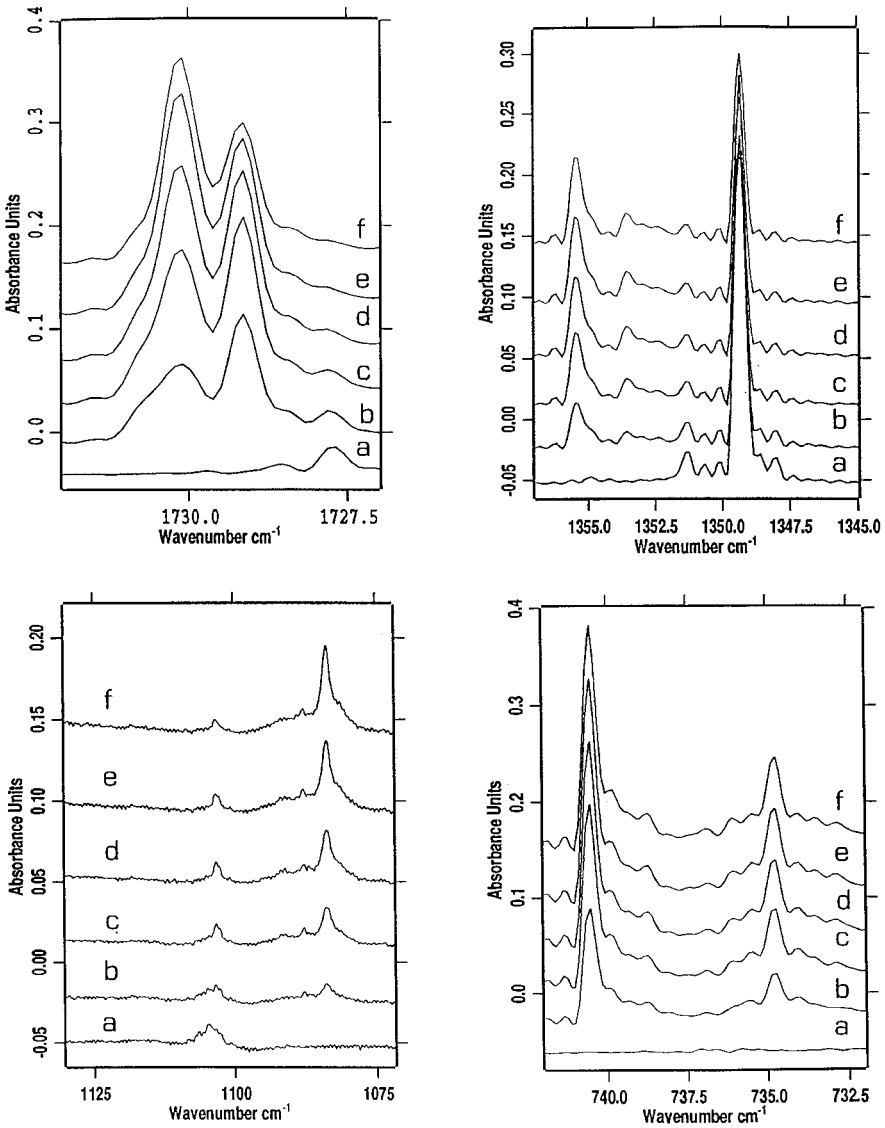

Figure 3. Product band growth during laser photolysis of a $CH_3Cl/O_3/Ar1/2/1000$ mixture in typical spectral regions below 2000 cm^{-1} with photolysis times of (a) 0, (b) 10, (c) 30, (d) 60, (e) 120, (f) 240 min.

When CD_3Cl was used instead of CH_3Cl, it showed a large deuterium shift and was located to 2480.5 cm^{-1}. An absorption measured at 3045.0 cm^{-1} which shifted to 2286.2 cm^{-1} with CD_3Cl was also observed near the $\nu^a_{CH_3}$ band of the methyl chloride parent molecule.

3000−2600 cm $^{-1}$ Region. New absorptions appeared at 2995.7, 2967.9, 2888.5, 2824.5, 2815.2−2813.2, and 2626.5−2620.5 cm^{-1}. The last band was relatively broad with a fwhm (full width half maximum) of 13 cm^{-1} and shifted, as did the doublet at 2815.3−2813.2 cm^{-1}, by a factor of 1.38 toward lower frequencies with CD_3Cl, suggesting that these bands belong to complexes involving the HCl molecule. In parallel, the bands at 2995.7, 2967.9, 2888.5, and 2824.5 cm^{-1} were shifted to 2224.2, 2158.5, 2206.0, and 2090 cm^{-1} with *H*/*D* isotopic shifts of 1.34, 1.37, 1.31, and 1.35, respectively, which suggest their assignment to either CH_3 or CH_2 groups. In isotopic ^{18}O enrichment, these bands appeared at about the same frequencies measured in CH_3Cl experiments.

2200−2100 cm $^{-1}$ Region. In the CO region, the doublet located at 2153.6−2151.0 cm^{-1} exhibited a 50 cm^{-1} ^{18}O shift and a 1.5 cm^{-1} D blue shift. Upon prolonged irradiation, after total disappearance of ozone, it continued to increase in a way similar to the behavior of the 2815.3−2813.2 cm^{-1} doublet.

1800−1650 cm $^{-1}$ Region. Photolysis of a CH_3Cl sample with 16 ozone gave a relatively strong doublet at 1730.1−1729.1 cm^{-1} in the carbonyl region with, in addition, a very weak feature at 1778.4 cm^{-1}, with this latter one disappearing upon prolonged photolysis. Upon deuterium substitution of methyl chloride, the strongest band was observed at 1683.7−1682.5 cm^{-1}, and in the $^{18}O_3$ experiments, it was located at 1697.2−1696.4 cm^{-1}, as illustrated in Figure 4.

1500−600 cm $^{-1}$ Region. Numerous weak bands were observed in this region. They were measured at 1497.2, 1446.4, 1400.8, 1372.9, 1355.4, 1321.1−1320.4, 1318.3, 1270.8, 1248.2, 1174.1, 1138.5, 1103.3, 1083.7, 1025.7, 815.3−808.8, 740.5−734.8, 689.9−686.1, and 672.9−669.3 cm^{-1}. Upon ^{18}O enrichment, a substantial shift was observed for the 1497.2, 1372.9, 1248.2, and 1083.7 cm^{-1} absorptions. They are then located at 1486.6, 1366.3, 1243.0, and 1057.2 cm^{-1}, respectively. The other bands showed only 1−2 cm^{-1} shifts toward the lower frequencies, except the 1138.5 cm^{-1} band that did not appear, indicating that this band is not a reaction product. In CD_3Cl experiments, all the observed bands with CH_3Cl were absent except the 1270.8 cm^{-1} feature. New weak bands were measured at 1149.0, 1098.0, 1064.0, 1055.2, 1027.1, 1018.0, 990.0, 962.0, 943.0, 843.4, 773.5, 769.0, and 709.5 cm^{-1}.

TABLE 3: Product Absorptions (cm^{-1}) after Photolysis of Natural and Isotopic $CH_3Cl/O_3/Ar$ Mixtures Using the 266 nm Laser Line[a]

$CH_3Cl + {}^{16}O_3$		$CH_3Cl + {}^{18}O_3$	$CD_3Cl + {}^{16}O_3$
$\lambda = 266$ nm	$\lambda = 532$ nm	$\lambda = 266$ nm	$\lambda = 266$ nm
3352.5 (0.02)		3341.0	2480.5
3045.0 (0.06)	3045.0	3044.6	2286.2
2995.7 (0.015)		2995.7	2224.2
2967.9 (0.2)	2967.9	2967.5	2158.5
2888.5 (0.03)		2888.4	2206.0
2824.5 (0.04)		2823.0	2090.0
2815.2−2813.2 (0.08)		2816.4−2814.4	2031.4
2626.5−2620.5 (0.9)		2625.5	1905.9−1901.6
2153.6−2151.0 (0.05)		2102.6−2101.9	2152.0
1869.7 (0.02)		1836.2	1869.4
1778.4 (0.005)		1730.0	
1730.1−1729.1 (0.3)		1697.2−1696.4	1683.7−1682.5
1497.2 (0.05)		1486.6	1098.0
1446.4 (0.15)	1446.4	1446.4	1055.2
1400.8 (0;003)			1064.7
1374.9 (sh)			
1372.9 (0.02)		1366.3	1149.0
1372.1 (sh)			
1355.4 (0.07)	1355.4	1355.5	1027.1
1321.1−1320.4 (0.01)		1319.0−1318.1	1018.0
1318.3 (0.004)	1318.3	1316.2	
1270.8 (0.025)		1269.8	1270.6
1248.2 (0.02)		1243.0	962.0
1174.1 (0.03)		1172.8	943.0
1103.3 (0.01)		1105.8	843.4
1083.7 (0.05)		1057.2	990.0
1025.7 (0.1)	1025.7	1024.9	773.5
815.3−808.8 (0.005)			769.0
740.5−734.8 (0.25)	740.5−734.8	739.3−733.6	709.5−703.1
689.9−686.1 (0.03)		686.3	
672.9−669.3 (0.03)	672.9−669.3	671.9−667.4	

[a] Integrated intensity in cm^{-1} measured after 120 mn irradiation time is indicated in brackets.

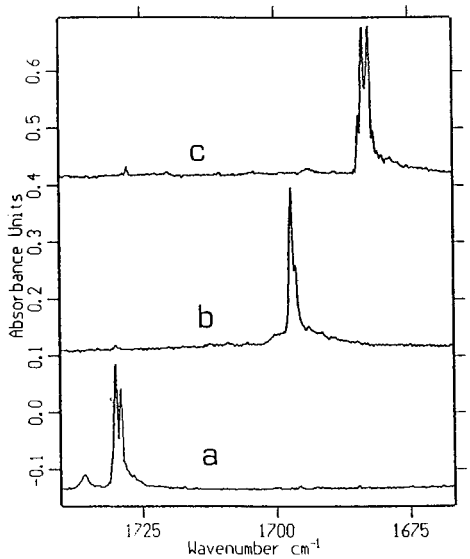

Figure 4. FTIR spectra of isotopic samples $CH_3Cl/O_3/Ar = 1/2/1000$ in the $\nu_{C=O}$ region after photolysis with the 266 nm laser line: (a) $CH_3Cl/O_3/Ar$; (b) $CH_3Cl/{}^{18}O_3/Ar$; (c) $CD_3Cl/{}^{16}O_3/Ar$.

4.2. Irradiation with the 532 nm Laser Line. Irradiation of a $CH_3Cl/O_3/Ar$ (1/2/1000) sample during 2 h at 25 K with the 532 nm laser line ($F = 6 \times 10^{17}$ photons cm^{-2} s^{-1}) was carried out. In regard to results obtained after 266 nm irradiation, major changes in the spectra occurred. Most of the bands observed with the 266 nm irradiation did not appear. Only absorptions at 3045.0, 2967.9, 1446.4, 1372.9, 1355.4, 1318.3, 1025.7, 740.5−734.8, and 672.9 cm^{-1} were observed. They appeared with a weaker intensity than that observed after 266 nm irradiation during the same time. Observation of these bands is the indication that one product at least is produced by reaction of CH_3Cl with ground-state atomic oxygen, whereas the other absorptions that are absent correspond to products formed by the reaction of excited oxygen with methyl chloride. Subsequent experiments were carried out with isotopic parent molecules. When CD_3Cl was substitued to CH_3Cl, new bands at 2286.2, 2158.5, 1027.1, 773.5, and 709.5 cm^{-1} were observed.

5. Identification of the Photoproducts

As a result of the weakness of the numerous bands that appear after irradiation, their assignment is not straightforward. However, on the basis of literature data, five sets of absorptions, which appeared only with the 266 nm irradiation, were relatively easily identified. A first set at 2815.3−2813.2 and 2153.6−2151.0 cm^{-1} was assigned to the hydrogen-bonded complex formed between the HCl molecule and the CO molecule, this assignment being supported by the isotopic shifts observed with CD_3Cl and $^{18}O_3$. The doublet at 2815.3−2813.2 cm^{-1} characterizes the stretching mode of the HCl submolecule (splitting due to chlorine isotope), whereas the 2153.6 cm^{-1} band corresponds to the stretching mode of the CO submolecule in the complex. Such a complex has been previously evidenced in an argon matrix.[27,28] A second set of bands, which appeared also only with the 266 nm irradiation, at 2888.5, 2824.5, 2626.5−2620.5, 1730.1−1729.1, 1497.2, 1248.2, and 1174.1 cm^{-1} was identified as resulting from the hydrogen-bonded complex between HCl and H_2CO by comparison with the matrix infrared spectrum of this species described by Nelander in solid nitrogen.[29] Only slight red frequency shifts were noted due to the different matrix environment. Thus, the broad band located around 2625 cm^{-1} characterizes the HCl submolecule complexed by H_2CO, whereas the other bands correspond to the ν_5, ν_1, ν_2, ν_3, ν_6, and ν_4 modes of the H_2CO submolecule in the complex, respectively. The shifts in these mode observed upon deuteration of CH_3Cl or with isotopic $^{18}O_3$ (not previously reported) agree well with the given assignments and the data are summarized in Table 4. In the ν_{CO} region, the additional very weak band that was measured at 1778.4 cm^{-1} and disappeared upon irradiation is tentatively assigned to the ν_{CO} stretching mode of the COHCl molecule previously identified by Nelander et al. in nitrogen.[30] Bands located to 1400.8 and 815.3−808.8 cm^{-1}, which disappeared upon prolonged photolysis, can be assigned to the H_2CCl radical on the basis of its spectra reported in the literature.[23,31] Their deuterium counterparts were tentatively assigned to the absorptions measured at 1064.0 and 769.0 cm^{-1}, respectively. Lastly, absorptions at 1869.7 and 1103.3 cm^{-1}, which shift to 1836.2 and 1105.8 cm^{-1} with $^{18}O_3$ and to 1869.4 and 843.4 cm^{-1} in CD_3Cl experiments, could be assigned to the ν_2 and ν_3 vibrational modes of the formyl radical (HCO) on the basis of its infrared detection by Pimentel et al.[32] Note that the 1103.3 cm^{-1} absorption is close to the ν_1 ozone absorption, but its identification as a photoproduct is not trivial because it is observed after the total disappearance of ozone.

Assignment of numerous other weak bands that appeared after irradiation was not straightforward. Comparison between spectra obtained after irradiation at 266 and 532 nm with, in addition, the evolution of bands after prolonged photolysis at 266 nm after disappearance of ozone or after temperature cycling allowed discrimination between several sets of bands. It appeared that there are two major products labeled hereafter A and B and several minor products.

Bands Labeled A. Bands at 3045.0, 2967.9, 1446.4, 1355.4, 1025.7, and 740.5−734.8 cm^{-1} appeared both with irradiation at 532 and 266 nm. They grew after annealing and were

TABLE 4: Observed Frequencies (cm^{-1}) of H_2CO/HCl Complex in Argon Matrix Compared with Nitrogen Matrix Frequencies from the Literature[29]

	N_2 matrix[29]	argon matrix (this work)		
assignment	H_2CO:HCl	H_2CO:HCl	$H_2C\ ^{18}O$:HCl	D_2CO:DCl
ν_1	2835.3, 2830.7	2824.5	2823.0	2090.2
ν_2	1727.3, 1725.8	1730.2, 1729.1	1697.2, 1696.4	1683.5, 1682.4
ν_3	1496.4	1497.2	1486.6	1099.1
ν_4	1178.1	1174.1	1172.8	943.0
ν_5	2900.0	2888.5	2888.4	2206.9
ν_6		1248.2	1247.5	962.0
ν_{HCl}	2591.0	2626.5, 2620.2	2625.5	1905.9, 1901.6

TABLE 5: Assignment of the Bands Labeled A Observed After Photolysis of $CH_3Cl/O_3/Ar$, $CH_3Cl/^{18}O_3/Ar$, and $CD_3Cl/O_3/Ar$ Mixtures with the 532 nm Laser Line

mode	$CH_3Cl^{16}O$	$CH_3Cl^{18}O$	$CD_3Cl^{16}O$
$\nu^a_{CH_3}$	3045.0	3044.6	2286.2
$\nu^s_{CH_3}$	2967.9	2967.9	2158.5
$\delta^a_{CH_3}$	1446.4	1446.4	1055.2
$\delta^s_{CH_3}$	1355.5	1355.5	1027.1
r_{CH_3}	1025.7	1025.7	773.5
ν_{CCl}	740.5−734.8	740.5−734.8	709.5−703.1

insensitive to prolonged photolysis at 266 nm. The position of all bands (Table 5) are close to those of the CH_3Cl molecule and are assigned by comparison to CH_3 stretching and deformation modes (symmetric and antisymmetric) and to a C−Cl stretching mode, respectively. The only product we can conceive from this assignment and that could emerge from the reaction of CH_3Cl with atomic oxygen is the CH_3ClO species, an isomer of CH_3OCl.

The infrared absorption spectrum of CH_3OCl between 3500 and 800 cm^{-1} has been recently reported.[33] It shows two predominant absorption features at 1006 and 2976 cm^{-1} and at least three relatively intense vibrations with resolved rotational structure between 1400 and 1500 cm^{-1}. As far as we know, the chlorosomethane, CH_3ClO, has not yet been identified, but the corresponding iodosomethane, CH_3IO, has been evidenced from photodissociation of an ozone complex with iodomethane.[34] As observed for the A species, in regard to the infrared spectrum of CH_3Cl, the infrared spectrum of iodosomethane parallels that of iodomethane quite closely.

Ab initio calculations of the structure and vibrational frequencies of the CH_3ClO singlet and triplet multiplicity species were carried out with the Gaussian 94 program.[35] They have been done with the correlation consistent polarized valence double-ζ (cc-pVDZ) basis set of Dunning and co-woker[36] at the B3-LYP level of theory (Becke three-parameter functional[37] and the nonlocal transformed correlation of Lee, Yang, and Parr,[38] as described in ref 39). Previous study showed that the B3-LYP (in conjonction with basis set of polarized double-ζ quality such as cc-pVDZ or higher) gives harmonic vibrational frequencies in good agreement with those computed as the CCSD(T) level.[39,40] Figures 5 and 6 report the optimized structures of singlet and triplet CH_3ClO. The CH_3Cl subunits in these species are very close to that of chloromethane calculated at the same level of theory except for the CCl bond length in the singlet species, which is stretched by about 0.03 Å. The singlet species can be regarded as being formed through a dative bond between one of the Cl lone pairs and the empty orbital in the (^{1}D) oxygen, given a ClO single bond while the triplet species is best regarded as a van der Waals (VDW) complex between triplet oxygen and CH_3Cl. The two lone electrons are still totally located on the oxygen.

Tables 6 and 7 report the calculated harmonic vibrational frequencies and IR intensities for selected isotopic species of

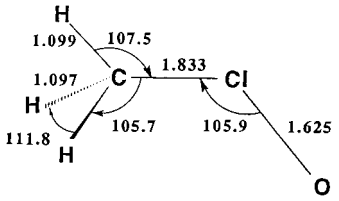

Figure 5. Calculated geometrical parameters of singlet CH_3ClO.

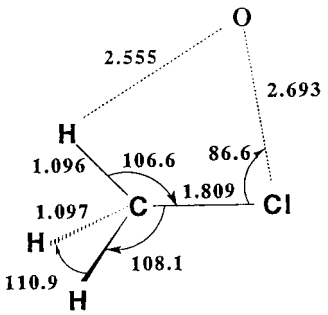

Figure 6. Calculated geometrical parameters of triplet CH_3ClO.

singlet and triplet CH_3ClO. As the species labeled A is observed when the reaction proceeds with (^{3}P) oxygen (irradiation at 532 nm), it should correspond to the CH_3ClO triplet species, which is about 4 kcal mol^{-1} lower in energy than the singlet species. The calculated most intense IR band corresponds to the CCl stretch predicted at 704 cm^{-1} for the most abondant isotopomer with an IR intensity of 30 km mol^{-1}. It is predicted somehow at a lower frequency than the observed one (740.5 cm^{-1}), but the calculated isotopic shifts agree nicely with the observed ones. They are 5, 0, and 30 cm^{-1} for ^{37}Cl, ^{18}O, and D, respectively, to be compared with the corresponding observed shifts of 5.7, 0, and 31 cm^{-1}. The same level of theory as used for CH_3Cl predicted the CCl stretch at 716 cm^{-1} to be lower than the argon matrix value of 722.5 cm^{-1}. The CCl stretch for the singlet species is predicted at 593 cm^{-1} with a small IR intensity (2 km mol^{-1}). A band is predicted at 725 cm^{-1} with an IR intensity of 26 km mol^{-1}, but the corresponding isotopic shift does not match the observed ones. In fact, this band corresponds to the ClO stretch. Thus, species A corresponds to the triplet CH_3-Cl···O complex and not to the chlorosomethane.

Recently, reaction of oxygen atoms with various bromomethanes in an argon matrix were reported.[41] With CH_3Br, ground-state atomic oxygen led only to traces of H_2CO···HBr, and the formation of CH_3Br···O species was not mentioned. To verify if absorptions corresponding to this species were present, we have irradiated a $CH_3Br/O_3/Ar$ (1/2/2000) mixture with 266 and 532 laser lines. New bands in the vicinity of the CH_3Br parent absorptions appeared after UV or visible irradiation that can be assigned to a complex between CH_3Br and the O(^{3}P) atom. Their positions are summarized in Table 8 and compared to those of CH_3Cl···O as well as those of iodosomethane. One can see that the frequency shifts of the CH_3Cl

TABLE 6: Calculated Isotopic Vibrational Frequencies (ν_i in cm^{-1}) and IR Intensities (I_i in km mol^{-1}) of Triplet CH_3ClO at the B_3LYP/cc-pVDZ Level[a]

	12−35−16−1		13−35−16−1	12−37−16−1	12−35−18−1	12−35−16−2		12−37−16−2		CH_3Cl 12−35−1
	ν_i	I_i	ν_i	ν_i	ν_i	ν_i	I_i	ν_i	description	ν_i
ν_1 (A′)	3195	≈0	3182	3195	3195	2374	≈0	2374	CH_3 a str	3066
ν_2	3070	21	3068	3070	3070	2194	15	2194	CH_3 s str	
ν_3	1445	6	1442	1445	1445	1047	3	1047	CH_3 a bend	
ν_4	1337	12	1331	1336	1337	1007	16	1007	CH_3 s bend	1350
ν_5	1010	4	1005	1010	1010	757	1	757	CH_3 rock	
ν_6	704	30	687	699	704	674	23	668	CCl str	
ν_7	140	2	140	140	135	138	4	138	ClO str	
ν_8	114	15	113	113	113	108	12	107	OClC bend	
ν_9 (A″)	3183	4	3171	3183	3183	2365	3	2365	CH_3 a str	3176
ν_{10}	1453	6	1450	1453	1453	1054	3	1054	CH_3 a bend	1441
ν_{11}	1012	3	1007	1012	1012	758	1	757	CH_3 rock	1008
ν_{12}	65	≈0	65	65	65	47	≈0	47	twist	

[a] For comparison calculated vibrational frequencies of 12-35-1 CH_3Cl at the same level are indicated in the last column.

TABLE 7: Calculated Isotopic Vibrational Frequencies (ν_i in cm^{-1}) and IR Intensities (I_i in km mol^{-1}) of Singlet CH_3ClO at the B_3LYP/cc-pVDZ Level[a]

	12−35−16−1		12−35−16−1	12−37−16−1	12−35−18−2	12−35−16−2		12−37−16−2		CH_3Cl 12−35−1
	ν_i	I_i	ν_i	ν_i	ν_i	ν_i	I_i	ν_i	description	ν_i
ν_1 (A′)	3186	1	3174	3186	3186	2368	≈0	2368	CH_3 a str	3066
ν_2	3055	7	3053	3055	3055	2180	4	2180	CH_3 s str	
ν_3	1441	9	1439	1441	1441	1046	5	1046	CH_3 a bend	
ν_4	1300	4	1294	1300	1300	984	3	984	CH_3 s bend	1350
ν_5	979	4	972	978	979	770	5	767	CH_3 rock	
ν_6	725	26	725	719	696	721	22	716	ClO str	
ν_7	593	2	579	588	593	557	2	553	CCl str	
ν_8	245	6	243	244	239	226	6	225	OClC bend	
ν_9 (A″)	3196	≈ 0	3184	3196	3196	2376	≈0	2376	CH_3 a str	3176
ν_{10}	1407	11	1404	1407	1407	1020	5	1020	CH_3 a bend	1441
ν_{11}	977	2	972	976	977	732	≈0	732	CH_3 rock	1008
ν_{12}	147	1	147	147	146	110	2	109	twist	

[a] For comparison calculated vibrational frequencies of 12-35-1 CH_3Cl at the same level are indicated in the last column.

TABLE 8: Comparison of Absorption Frequencies (cm^{-1}) of $CH_3Br\cdots O$ and $CH_3Cl\cdots O$ with Those of CH_3Br and CH_3Cl and Comparison of CH_3IO Absorption Frequencies in Frequencies with CH_3I Absorption

	CH_3Br	$CH_3Br\cdots O$	CH_3Cl	$CH_3Cl\cdots O$	CH_3I[34]	CH_3IO[34]
ν_1 ($\gamma^S_{CH_3}$)	2967.0	2971.5	2965.1	2967.92	2965.7	2945.3
ν_2 ($\delta^S_{CH_3}$)	1300.1	1307.5−1306.2	1349.4	1355.5	1245.5	1223.4
ν_3(C−X)	602.8−601.6	624.3−623.2	722.4−716.7	740.8−734.8	527.8	496.6
ν_4 ($\gamma^a_{CH_3}$)	3054.6	3060.4	3040.8	3045.0		
ν_5 ($\delta^a_{CH_3}$)	1436.7	1438.1	1445.5	1446.4	1431	1400.3
ν_6 (r_{CH_3})	952.1	264.7	1015.0	1025.7	880.4	848.0−858.9
ν_{O-X}		577.3−576.6				723.7

and CH_3Br bands in the complex in regard to the corresponding monomers bands are comparable. On the other hand, the CH_3-IO absorptions are red shifted with respect to the CH_3I bands, whereas in the $CH_3X\cdots O$ complexes (X = Cl,Br), they are blue shifted from CH_3X absorptions. Furthermore, the position of the ν_{IO} band (723.7 cm) is in agreement with the caculated position of the Cl−O band in the singlet CH_3ClO species (chlorosomethane).

Group of Bands Labeled B. Bands at (3352.5, 2995.7, 1372.9, 1321.1−1320.4, 1083.7, and 689.9−686.1 cm^{-1} appeared only after irradiation at 266 nm. They grew upon prolonged irradiation after the disappearance of ozone, suggesting that they characterize a secondary reaction product. They are tentatively assigned to the chloromethanol CH_2OHCl molecule on the basis of the following arguments and literature data.[42,43] The absorption at 3352.5 cm^{-1} is characteristic of an OH group, a conclusion supported by its shift to 2480.5 cm^{-1} on deuteration of methyl chloride. Its position at a lower frequency than that of free OH groups suggests intramolecular hydrogen bonding between OH and chlorine atoms comparable to that observed for the iodomethanol between the iodine atom and OH group.[34] The position of the band at 1083.7 cm^{-1} with its 28 cm^{-1} ^{18}O isotopic shift seems to indicate the presence of a C−O bond in species B. On deuteration, this band is displaced to 990 cm^{-1}, an expected shift due to mixing with CD_2 modes as observed for CH_2OHCN[44] and CH_2OHCCl_3.[45] Absorptions at 2995.7 cm^{-1} and 1321.1−1320.4 cm^{-1}, which show a large deuterium shift, could be responsible for a CH_2 stretching mode and an out-of-plane bending CH_2 mode, respectively, whereas the band at 1372.9 cm^{-1} showing an ^{18}O shift of 6.5 cm^{-1} and a large deuterium shift can be assigned to the C−O−H bending. Lastly, the doublet at 689.9−686.1 cm^{-1}, which shows a weak shift with ^{18}O, could be candidate for a CCl stretching mode.

One other group of weak bands that appeared both with 532 and 266 nm laser line irradiation, namely absorptions at 1318.0 and 672.9−669.3 cm^{-1}, remained unidentified.

6. Photolytic Process

6.1. Growth Behavior of the Product. A series of photolysis experiments with the 266 nm laser line were performed after

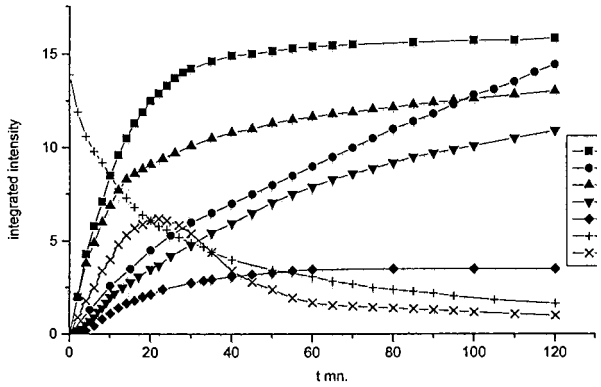

Figure 7. Time evolution of photoproducts and ozone after photolysis of a $CH_3Cl/O_3/Ar$ mixture (1/2/1000) with the 266 nm laser line (integrated intensities (*I*) are multiplicated by arbitrary constants).

several irradiation times to find primary and secondary products formed from the $CH_3Cl + O_3$ reaction. Figure 7 presents the curves obtained from integrated intensity measurements of one characteristic band of each set of photoproducts. The intensities of the bands were multiplied with arbitrary constants to make them comparable. The depletion of ozone with time in the same experiment was also represented using the ν_3 ozone band. Distinct behaviors are evidenced among the different photoproducts. Product bands of H_2CO/HCl, $CH_3Cl\cdots O$, and CH_2Cl grow rapidly at short time then approach a constant value (H_2CO/HCl, $CH_3Cl\cdots O$) or decrease (CH_2Cl) after nearly all the ozone is depleted, indicating that they are primary products of the reaction. In contrast, bands of CH_2OHCl and HCO product species have a sigmoidal contour with near zero slope at short times and continue to increase after ozone depletion, indicating they arise from secondary chemistry. The product band of $CO\cdots HCl$ at 2153.6 cm^{-1} increases also upon prolonged photolysis, but at short times, it grows strongly, suggesting it belongs to both primary and secondary photoproducts.

6.2. Reaction of $O(^3P)$ Atom. Reaction of ground-state atomic oxygen with methyl chloride can proceed according two mechanisms: (i) abstraction of chlorine or hydrogen atoms from CH_3Cl or (ii) addition of the oxygen atom to the CH_3Cl molecule, which can be combined with a simultaneous fragmentation of the initial adduct. In the matrix cage, photofragments can recombine and abstraction of a H or Cl atom by atomic oxygen can lead to the appearance of CH_2OHCl or CH_3OCl. No absorptions assignable to one or another of these species were obtained after irradiation with the 532 nm laser line. Observation of bands characterizing $CH_3Cl\cdots O$ as a primary product seems to indicate that there is addition of the oxygen atom to the chlorine atom of CH_3Cl. In the gas-phase, an addition mechanism as the major channel has been also reported for the reaction of oxygen atom with alcene[46] and sulfur compounds,[47] with the addition leading to an intermediate complex in a first step. No carbonyl products were formed as observed with CH_3Br.[41]

6.3. Reaction of the $O(^1D)$ Atom. The major product of the reaction of $O(^1D)$ with methyl chloride is the formaldehyde (H_2CO), which appears to be complexed by HCl produced in parallel in the matrix cage. Formation of carbonyl compounds as major products by HCl elimination was also observed from the reaction between $O(^1D)$ and other halocarbons containing hydrogen atoms. Thus, $COCl_2$ and COHCl were identified as primary products of the reaction of excited atomic oxygen with $CHCl_3$[10] and CH_2Cl_2,[13] respectively. At first sight, the presence of $ClCH_2OH$ (bands B) could suggest that the formaldehyde molecule occurs from an insertion−elimination reaction as follows:

$$O(^1D) + CH_3Cl \rightarrow [ClCH_2OH]^* \rightarrow HCl + Cl_2CO \quad (1)$$

Insertion of excited atomic oxygen in a CH bond has been previously evidenced for CH_4,[42] CH_3OH,[48] CH_3CCl_3,[14] and CH_3CN.[44] As a result of the condensed matter, a weak yield of excited $[ClCH_2OH]^*$ can be deactivated, explaining its identification. However, the growth of the formaldehyde molecule and that of $ClCH_2OH$ are not in agreement with this assumption, and eq 1 is not likely. Formaldehyde appears as a primary product, while chloromethanol appears as a secondary product and grows under irradiation after the disappearance of ozone. The formaldehyde is probably formed by a direct attack of atomic oxygen upon the carbon of the chloromethane leading to a five-centered highly excited intermediate, which subsequently fragments leading to $CH_2O\cdots HCl$ and perhaps to $HCOCl$ and $CO\cdots HCl$ products, which have been also observed. The HCOCl produced as traces is sensitive to the irradiation and decomposes into $CO\cdots HCl$. However, as previously noted, the growth curve of $CO\cdots HCl$, which does not show a sigmoidal contour at short time, is the indication that the CO−HCl complex is also produced as a primary product, as observed in the case of CH_2Cl_2[13] and suggested in the case of $CHCl_3$ by the growth of HCl.[10]

The $CH_3Cl\cdots O$ complex, which is observed after ozone irradiation at 532 nm, appears in a considerable greater yield after ozone irradiation at 266 nm. It is probably formed by addition of $O(^3P)$ formed after quenching of $O(^1D)$. After annealing, diffusion of $O(^3P)$ atoms in the matrix explains the growth of $CH_3Cl\cdots O$.

Identification of the chloromethyl radical CH_2Cl indicates abstraction by an $O(^1D)$ atom of a hydrogen atom from methyl chloride as suggested in the gas phase.[9] As a result of the cage effect, this minor channel in the matrix could lead to CH_2OHCl by recombination of the two photofragments.

$$CH_3Cl + O(^1D) \rightarrow CH_2Cl + OH \rightarrow ClCH_2OH \quad (2)$$

The OH radical, which is the expected product with CH_2Cl, was not detected, perhaps because of the weakness of the OH band or of its reaction with an oxygen atom ($O + OH \rightarrow H + O_2$).

Conclusion

The photolysis of O_3 in argon containing chloromethane can be summarized as follows:

$$CH_3Cl + O(^3P) \rightarrow CH_3Cl\cdots O$$

$$+ O(^1D) \rightarrow \begin{cases} CH_2C=O\cdots HCl \\ CO\cdots HCl + H_2 \\ CH_2Cl + OH \rightarrow CH_2ClOH \\ CHClO + H_2 \end{cases}$$

With $O(^1D)$ the major channel is the formation of formaldehyde, which appears to be complexed with hydrogen chloride in the matrix cage. The most striking result is the formation of a $CH_3X\cdots O$ complex (X = Cl, Br). Identification of this species stabilized in the matrix suggests that, in the gas phase, the reaction of ground-state atomic oxygen with chloro- and bromo-

methanes probably proceeds by this intermediate, which subsequently fragments into CH_3 and O or CH_2 and OH radicals.

References and Notes

(1) Talukdar, R. K.; Mellouki, A.; Schmoltner, A. M.; Watson, T.; Montzka, S.; Ravishankara, A. R *Science* **1992**, *257*, 229.

(2) Talkdar, R.; Mellouki, A.; Gierezak, T.; Burkholder, J. B.; McKeen, S. A.; Ravishankara, A. R. *J. Phys. Chem*. **1991**, *95*, 5815.

(3) Zhang, Z.; Huie, R. E.; Kurylo, M. J. *J. Phys. Chem*. **1992**, *96*, 1533.

(4) Moore, S. B.; Carr, R. W. *J. Phys. Chem*. **1990**, *94*, 1393.

(5) Wu, F.; Carr, R. W. *J. Phys. Chem*. **1992**, *96*, 1743.

(6) T. J.; Hurley, M. D.; Nielsen, O. J.; Sehested, J. *J. Phys. Chem*. **1994**, *98*, 5686.

(7) Mogelberg, T. E.; Nielsen, O. J.; Sehested, J.; Wallington, T. J.; Hurley, M. D.; Schneider, W. F. *Chem. Phys. Lett*. **1994**, *225*, 375.

(8) Wallington, T. J.; Sehested, J. J.; Nielsen, O. J. *Chem. Phys. Lett*. **1994**, *226*, 563.

(9) Weller, R.; Lorenzen-Schmidt, H.; Schrems, O. *Ber. Bunsen-Ges. Phys. Chem*. **1992**, *96*, 4090.

(10) Schriver-Mazzuoli, L.; Gauthier-Roy, B.; Carrere, D.; Schriver, A.; Abouaf-Marguin, L. *Chem. Phys*. **1992**, *163*, 357.

(11) Abdelaoui, O.; Schriver-Mazzuoli, L.; Schriver, A. *J. Mol. Struct*. **1992**, *268*, 335.

(12) Schriver-Mazzuoli, L.; Abdelaoui, O.; Schriver, A. *J. Phys. Chem*. **1992**, *96*, 8069.

(13) Lugez, C.; Schriver, A.; Lasson, E.; Nielsen, C. J.; Schriver-Mazzuoli, L. *J. Phys. Chem*. **1993**, *97*, 11617.

(14) Pettersen, V.; Schriver-Mazzuoli, L.; Schriver, A.; Chaquin, P.; Lasson, E. *Chem. Phys*. **1996**, *204*, 115.

(15) Clark, R. J. H.; Dann, J. R. *J. Phys. Chem*. **1996**, *100*, 9271.

(16) Schriver-Mazzuoli, L.; Schriver, A.; Lugez, C.; Perrin, A.; Camy-Peyret, C.; Flaud, J. M. *J. Mol. Spectrosc*. **1996**, *176*, 85.

(17) Tanabe, K.; Saëki, S. *Spectrochim. Acta* **1970**, *26*, 1469.

(18) Henfrey, N. F.; Trush, B. A. *J. Mol. Struct*. **1986**, *146*, 71.

(19) Betrencourt, M.; Morillon-Chapey, M.; Blanquet, G.; Warland, J. *J. Mol. Spectrosc*. **1988**, *128*, 433.

(20) Bouanich, J. P.; Blanquet, G.; Warland, J. *J. Mol. Spectrosc*. **1993**, *161*, 416.

(21) Demaison, J.; Bocquet, R.; Chen, W. D.; Papousek, D.; Boucher, D.; Burger, H. *J. Mol. Spectrosc*. **1994**, *166*, 147.

(22) King, S. T. *J. Chem. Phys*. **1968**, *49*, 1521.

(23) Andrews, L.; Smith, D. W. *J. Chem. Phys*. **1970**, *53*, 2956.

(24) Benderski, A. V.; Wight, C. A. *J. Chem. Phys*. **1994**, *101*, 292.

(25) Bahou, M.; Schriver-Mazzuoli, L.; Camy-Peyret, C.; Schriver, A. *Chem. Phys. Lett*. **1997**, *273*, 31.

(26) Bahou, M.; Schriver-Mazzuoli, L.; Camy-Peyret, C.; Schriver, A.; Chiavassa, T.; Aycard, J. P. *Chem. Phys. Lett*. **1997**, *265*, 145.

(27) Andrews, L.; Arlinghaus, R. J.; Johnson, C. L. *J. Chem. Phys*. **1983**, *78*, 6348.

(28) Perchard, J. P.; Cipriani, J.; Silvi, B.; Maillard, D. *J. Mol. Struct*. **1983**, *100*, 317.

(29) Nelander, B. *J. Mol. Struct*. **1980**, *69*, 59.

(30) Stradman-Long, L.; Nelander, B.; Nord, L. *J. Mol. Struct*. **1984**, *117*, 217.

(31) Jacox, M. E.; Milligan, D. E. *J. Chem. Phys*. **1970**, *53*, 2688.

(32) Ewing, G. E.; Thompson, E.; Pimentel, G. C. *J. Chem. Phys*. **1960**, *32*, 927.

(33) Crowley, J. N.; Helleis, F.; Muller, R.; Moortgat, G.; Crutzen, P. J. *J. Geophys. Res*. **1994**, *99*, 20683.

(34) Hawkins, M.; Andrews, L. *Inorg. Chem*. **1985**, *24*, 3285.

(35) Frisch, M. J.; Trucks, G. W.; Schlegel, H. B.; Gill, P. M. W.; Johnson, B. G.; Robb, M. A.; Cheeseman, J. R.; Keith, T.; Petersson, G. A.; Montgomery, J. A.; Raghavachari, K.; Al-Laham, M. A.; Zakrzewski, V. G.; Ortiz, J. V.; Foresman, J. B.; Cioslowski, J.; Stefanov, B. B.; Nanayakkara, A.; Challacombe, M.; Peng, C. Y.; Ayala, P. Y.; Chen, W.; Wong, M. W.; Andres, J. L.; Replogle, E. S.; Gomperts, R.; Martin, R. L.; Fox, D. J.; Binkley, J. S.; Defrees, D. J.; Baker, J.; Stewart, J.; Head-Gordon, M.; Gonzalez, C.; Pople, J. A. *Gaussian 94*, revision B.1; Gaussian Inc.: Pittsburgh, PA, 1995.

(36) Woon, D. E.; Dunning, T. H., Jr. *J. Chem. Phys*. **1993**, *98*, 1358. Dunning, T. H., Jr. *J. Chem. Phys*. **1989**, *90*, 1007.

(37) Becke, A. D. *J. Chem. Phys*. **1993**, *98*, 5648.

(38) Lee, C.; Yang, W.; Paar, R. G. *Phys. Rev*. **1988**, *B37*, 785.

(39) Stevens, P. J.; Devlin, F. J.; Chabalowski, C. F.; Frish, M. J. *J. Phys. Chem*. **1994**, *98*, 11623.

(40) Martin, J. M. L.; El Yazal, J.; François, J. P. *Mol. Phys*. **1995**, *86*, 1437. Devlin, F. J.; Finley, J. W.; Stevens, P. J.; Frish, M. J. *J. Phys. Chem*. **1995**, *99*, 16883. Rahut, G.; Pulay, P. *J. Phys. Chem*. **1995**, *99*, 3093. Wong, M. W. *Chem. Phys. Lett*. **1996**, *256*, 391.

(41) Lasson, E.; Nielsen, C. J. *Acta Chem. Scand*. **1997**, *51*, 1.

(42) Kunttu, H.; Dahlquist, M.; Murto, J.; Rasanen, M. *J. Phys. Chem*. **1988**, *92*, 1495.

(43) Tyndall, G. S.; Wallington, T. J.; Hurley, M. D.; Scneider, W. F. *J. Phys. Chem*. **1993**, *97*, 576.

(44) Mielke, Z.; Hawkins, M.; Andrews, L. *J. Phys. Chem*. **1989**, *93*, 558.

(45) Pertilla, M. *Spectrochim. Acta* **1979**, *35A*, 585.

(46) Huang, X.; Xing, G.; Bersohn, R. *J. Chem. Phys*. **1994**, *101*, 5818.

(47) Cvetanovic, R. J.; Singleton, D. L.; Irwin, R. S. *J. Am. Chem. Soc*. **1981**, *103*, 3530.

(48) Lugez, C.; Schriver, A.; Levant, R.; Schriver-Mazzuoli, L. *Chem. Phys*. **1994**, *181*, 129.